Planta (2021) 254:131
https://doi.org/10.1007/s00425-021-03794-y

ORIGINAL ARTICLE

Functional analysis of GT61 glycosyltransferases from grass species in xylan substitutions

Ruiqin Zhong[1] · Dongtao Cui[2] · Dennis R. Phillips[3] · Nathanael T. Sims[1] · Zheng-Hua Ye[1]

Received: 19 August 2021 / Accepted: 16 November 2021 / Published online: 25 November 2021

Abstract

Main conclusion **Multiple rice GT61 members were demonstrated to be xylan arabinosyltransferases (XATs) mediating 3-*O*-arabinosylation of xylan and the functions of XATs and xylan 2-*O*-xylosyltransferases were shown to be conserved in grass species.**

Abstract Xylan is the major hemicellulose in the cell walls of grass species and it is typified by having arabinofuranosyl (Ara*f*) substitutions. In this report, we demonstrated that four previously uncharacterized, Golgi-localized glycosyltransferases residing in clade A or B of the rice GT61 family were able to mediate 3-*O*-arabinosylation of xylan when heterologously expressed in the Arabidopsis *gux1/2/3* triple mutant. Biochemical characterization of their recombinant proteins established that they were xylan arabinosyltransferases (XATs) capable of transferring Ara*f* residues onto xylohexaose acceptors, and thus they were named OsXAT4, OsXAT5, OsXAT6 and OsXAT7. OsXAT5 and the previously identified OsXAT2 were shown to be able to arabinosylate xylooligomers with a degree of polymerization of as low as 3. Furthermore, a number of XAT homologs from maize, sorghum, *Brachypodium* and switchgrass were found to exhibit activities catalyzing Ara*f* transfer onto xylohexaose, indicating that they are XATs involved in xylan arabinosylation in these grass species. Moreover, we revealed that homologs of another GT61 member, xylan 2-*O*-xylosyltransferase (XYXT1), from these grass species could mediate 2-*O*-xylosylation of xylan when expressed in the Arabidopsis *gux1/2/3* mutant. Together, our findings indicate that multiple OsXATs are involved in 3-*O*-arabinosylation of xylan and the functions of XATs and XYXTs are conserved in grass species.

Keywords Arabinosyltransferase · Cell wall · Xylan · XAT · XYXT

Introduction

The grass family is one of the largest and most widely distributed plant families and it is vital to humanity since the cultivated grasses, including maize, rice and wheat, are the most extensively grown food crops (Levetin and McMahon 2016). In addition, some grass species, such as switchgrass, sorghum and miscanthus, have been exploited to be promising sources of lignocellulosic biomass for second generation biofuel production (Marriott et al. 2016). One of the major biopolymers in grass biomass is xylan, which is a polysaccharide that is crosslinked with lignin through hydroxycinnamates in grass species. The xylan–lignin crosslinking is considered to be one of the factors contributing to the recalcitrance of grass biomass conversion into fermentable sugars for biofuel generation as well as to the low digestibility of grass species used for animal feeding (Buanafina 2009; Hatfield et al. 2017). Therefore, uncovering the biochemical mechanisms controlling xylan biosynthesis in grass species could potentially provide a knowledge base for genetically modifying grass biomass composition tailored for diverse end uses.

Xylan is the major hemicellulose in both primary and secondary walls of grass species. The backbone xylosyl (Xyl) residues of grass xylan are substituted extensively with

Communicated by Anastasios Melis.

✉ Zheng-Hua Ye
yh@uga.edu

[1] Department of Plant Biology, University of Georgia, Athens, GA 30602, USA

[2] Department of Chemistry and Chemical Biology, Harvard University, Cambridge, MA 02138, USA

[3] Department of Chemistry, University of Georgia, Athens, GA 30602, USA

3-*O*-arabinofuranosyl (Ara*f*) residues but only slightly with glucuronic acid/methylglucuronic acid (GlcA/MeGlcA), which differs from dicot xylan that is characterized by having GlcA/MeGlcA as the major substituents (Vogel 2008). Depending on grass species, the 3-*O*-Ara*f*-substituted backbone Xyl residues could be further arabinosylated at *O*-2 forming 2,3-di-*O*-Ara*f* substitutions, and the 3-*O*-Ara*f* side-chain residues could be further decorated at *O*-2 with Ara*f* or Xyl to generate the disaccharide side chains Ara*f*–Ara*f* or Xyl–Ara*f*, respectively (Hoffmann et al. 1991; Verbruggen et al. 1998; Höije et al. 2006; McCleary et al. 2015). The 3-*O*-Ara*f* side-chain residues could also be substituted at *O*-5 with hydroxycinnamates, such as ferulic acid or *p*-coumaric acid, which are involved in crosslinking xylan as well as xylan with lignin in grass species (Hartley et al. 1990; Ralph et al. 1995). In addition to the sugar and hydroxycinnamate substituents, grass xylan is often acetylated at *O*-2 and *O*-3 of the backbone Xyl residues (Naran et al. 2009; Carvalho et al. 2017; Zhong et al. 2018a).

Genetic analyses have demonstrated that the backbone elongation of grass xylan entails glycosyltransferases (GTs) from the GT43 and GT47 families, which is the same as that of dicot xylan (Zeng et al. 2010; Chiniquy et al. 2013; Lovegrove et al. 2013; Lee et al. 2014; Urbanowicz et al. 2014; Zhang et al. 2014; Whitehead et al. 2018; Pellny et al. 2020; Petrik et al. 2020). Several glycosyltransferases in the GT61 family have been implicated in the 3-*O*-Ara*f* substitutions of grass xylan. It was shown that downregulation in the expression of wheat xylan arabinosyltransferase 1 (TaXAT1) caused a major reduction in xylan 3-*O*-Ara*f* substitutions in the endosperm, and TaXAT2 and rice OsXAT2/3 could arabinosylate xylan when heterologously expressed in Arabidopsis (Anders et al. 2012). OsXAT2 was biochemically proven to be a 3-*O*-arabinosyltransferase catalyzing 3-*O*-Ara*f* transfer onto xylan (Zhong et al. 2018b) and double knockout mutations of OsXAT2/3 caused a reduction in arabinosyl content in rice cell walls (Chen et al. 2021). Two other rice GT61 members, XAX1 (xylosyl arabinosyl substitution of xylan 1) and OsXYXT1 (xylan 2-*O*-xylosyltransferase 1), are also involved in xylan substitutions. Mutation of the *XAX1* gene led to an absence of the fingerprinting peak corresponding to the Xyl–Ara*f* side chains of xylan and thus, it was proposed to mediate Xyl transfer onto xylan, but its exact biochemical function remains elusive (Chiniquy et al. 2012). OsXYXT1 was demonstrated to be a β-1,2-xylosyltransferase catalyzing the transfer of 2-*O*-Xyl side chains directly onto the xylan backbone as evidenced by its heterologous expression in the Arabidopsis *gux1/2/3* mutant and activity assays of its recombinant protein (Zhong et al. 2018b). Hydroxycinnamate esterification of the Ara*f* side chains of grass xylan was proposed to be mediated by a group of grass-specific BAHD acyltransferases (Mitchell et al. 2007; Pellny et al. 2012). Overexpression or downregulation in the expression of a number of these BAHD genes in rice, *Brachypodium*, sugarcane and *Setaria viridis* have been shown to result in an alteration in the level of hydroxycinnamates associated with hemicelluloses (Piston et al. 2010; Bartley et al. 2013; Buanafina et al. 2016; de Souza et al. 2018; Fanelli et al. 2021; Mota et al. 2021). Like that of dicot xylan, the acetylation of grass xylan is catalyzed by a group of DUF231 domain-containing acetyltransferases (Gao et al. 2017; Zhong et al. 2018a, 2019).

Glycosyltransferases in the GT61 family have been phylogenetically grouped into three clades named A, B, and C, and clade A had undergone a substantial expansion in grass species, e.g., there are 19 clade A members in rice versus only 2 in Arabidopsis (Mitchell et al. 2007; Anders et al. 2012). As described above, thus far only several clade A members, including four rice ones (OsXAT2/3, XAX1 and OsXYXT1) and two wheat ones (TaXAT1/2), have been shown to be involved in xylan substitutions. In this report, we performed a comprehensive functional analysis of rice GT61 members for their involvement in xylan substitutions by heterologous expression in the Arabidopsis *gux1/2/3* mutant. Three new members (OsXAT4/5/6) in clade A and one member (OsXAT7) in clade B of the rice GT61 family were found to mediate the addition of 3-*O*-Ara*f* side chains onto xylan. We further revealed that the recombinant proteins of OsXATs and their homologs from maize, sorghum, *Brachypodium* and switchgrass were able to add one to three Ara*f* residues onto the xylohexaose acceptors, which provides unequivocal biochemical evidence demonstrating that they are xylan arabinosyltransferases. In addition, we showed that XYXT1 homologs from these grass species were capable of transferring 2-*O*-Xyl side chains onto xylan when expressed in the Arabidopsis *gux1/2/3* mutant. These findings not only enrich our understanding of the functional roles of GT61 members in grass xylan substitutions but also provide molecular tools for modifying xylan structure in biofuel crops such as switchgrass.

Materials and methods

Phylogenetic analysis

The amino acid sequences of Rice GT61 proteins were retrieved from the genome sequence database of rice (*Oryza sativa* v7_JGI at Phytozome v12). OsXATs and OsXYXT1 were used to BLAST search for their close homologs from the genome sequence databases *of* maize (*Zea mays*), sorghum (*Sorghum bicolor*), *Brachypodium distachyon* and switchgrass (*Panicum virgatum*) at Phytozome v12. Their phylogenetic relationship was evaluated using the MEGA (v6.0) software with the maximum likelihood method.

Generation of transgenic *gux1/2/3* plants expressing grass GT61 genes

The full-length GT61 cDNAs from rice, maize, sorghum, *Brachypodium distachyon* and switchgrass were PCR-amplified and confirmed by sequencing. The cDNAs were inserted between the 2-kb *AtCesA7* promoter and the nopaline synthase terminator in a modified pGPTV-HPT binary vector to create the GT61 expression constructs, which were introduced into the Arabidopsis *gux1/2/3* mutant plants by *Agrobacterium*-mediated transformation. For each construct, three separate pools of stems, each from at least 20 independent transgenic plants, were used as three biological replicates for subsequent structural analyses of xylan.

Generation of xylooligomers by xylanase digestion

Stems collected from the transgenic plants were ground into powders in liquid nitrogen and the alcohol-insoluble cell walls were isolated as previously described (Zhong et al. 2005). The cell walls were first extracted with ammonium oxalate to remove pectin and then extracted with 1 N KOH for xylan, which was digested with endo-1,4-β-xylanase M6 (GH11; Megazyme, Wicklow, Ireland). The xylanase-released xylooligomers were passed through a Sephadex G25 column (1 × 100 cm) and eluted with H_2O. Carbohydrates in the eluent were monitored by a refractive index detector and the fractions containing xylooligomers were pooled and lyophilized before analysis. Since the xylan reducing end oligosaccharide and the substituted xylotetraose oligomers, if present, were eluted in proximate fractions as reported previously (Zhong et al. 2018b), they were pooled together and analyzed as a mixture. Although in a mixture, the identities of the xylan reducing end oligosaccharide and the substituted xylotetraose oligomers could be readily distinguished using nuclear magnetic resonance (NMR) based on their chemical shifts (Pena et al. 2007; Zhong et al. 2018b).

MALDI-TOF mass spectrometry

Matrix-assisted laser desorption ionization-time-of-flight (MALDI-TOF) mass spectrometry was carried out using a Bruker Autoflex TOF mass spectrometer (Billerica, MA, USA) in reflection mode. The samples were mixed (1:1, v/v) with the MALDI matrix (0.1 M 2,5-dihydroxybenzoic acid and 0.03 M 1-hydroxyisoquinoline in 50% acetonitrile) and dried on a target plate. One microliter of xylanase-released xylooligomers (1 μg/μl) or the XAT-catalyzed reaction mixtures were used for analysis. The spectra were the averages of at least 100 laser shots. Xylooligomers isolated from three separate pools of stems for each construct were analyzed and representative spectra were shown.

NMR spectroscopy

One-dimensional (1D) and two-dimensional (2D) NMR spectra of the isolated xylooligomers were recorded using standard Varian pulse sequences with a Varian Inova 500 MHz spectrometer (Varian Inc., Palo Alto, CA, USA). The proton positions and residue identities in the NMR spectra were assigned based on our 1D and 2D NMR spectral data and the published NMR spectral data for xylan (Pena et al. 2007; Chiniquy et al. 2012; McCleary et al. 2015; Zhong et al. 2018b).

Generation of recombinant XAT proteins

Recombinant XAT proteins were heterologously expressed in the human embryonic kidney (HEK) 293 cells in a secreted form. Briefly, the XAT cDNAs with deletion of the N-terminal transmembrane helix were ligated in frame between the murine Igκ chain leader sequence (for protein secretion) and the c-myc epitope and six tandem histidine tag in the pSecTag2 mammalian expression vector (Invitrogen, Waltham, MA, USA). The amino acids used for recombinant protein production were from numbers 40 to 583 for OsXAT2, 40 to 576 for OsXAT3, 36 to 460 for OsXAT4, 36 to 485 for OsXAT5, 39 to 500 for OsXAT6, 48 to 491 for OsXAT7, 40 to 596 for ZmXAT1, 33 to 455 for ZmXAT2, 35 to 462 for SbXAT1, 36 to 501 for BdXAT1, 40 to 593 for PvXAT1, 41 to 596 for PvXAT2, and 40 to 573 for PvXAT3. The expression constructs were transfected into HEK293 cells using the Invitrogen FreeStyle 293 Expression System according to the manufacturer's protocol. After 5 days of culture, the culture media were collected for purification of expressed proteins by passing through a nickel resin column. The purified proteins were examined by sodium dodecyl sulfate-polyacrylamide gel electrophoresis (SDS-PAGE) followed by Coomassie Blue staining.

Arabinosyltransferase activity assay

Xylan arabinosyltransferase activity was assayed by incubating the purified recombinant XAT proteins (20 μg) with 0.3 mM UDP-Ara*f* (Peptide Institute, Osaka, Japan), 0.3 mM anthranilic acid (AA)-labeled xylooligomers, and 1 mM $MgCl_2$ in 50 mM HEPES buffer (pH 7.0) at 37 °C for 4 h. Xylooligomers (Xyl_3 to Xyl_6; Megazyme) were labeled at their reducing termini with AA (Ishii et al. 2002). The addition of Ara*f* residues on the xylooligomer acceptors in the XAT-catalyzed reaction products was examined with MALDI-TOF mass spectrometry.

Subcellular localization

OsXATs tagged with green fluorescent protein (GFP) at their C-terminus were cloned under the cauliflower mosaic virus 35S promoter in a modified pBI221vector. These constructs were co-transfected with a construct expressing mCherry-tagged FRA8 (Zhong et al. 2005) into Arabidopsis leaf protoplasts (Yoo et al. 2007). The fluorescent signals in the transfected protoplasts were recorded using a Zeiss LSM 710 confocal microscope. At least 10 Arabidopsis protoplasts were imaged and representative images were shown.

Statistical analysis

Three independent biological replicates were conducted for each of the experiments reported in this study and representative spectra of the MALDI-TOF MS and NMR data were shown.

Accession numbers

The GenBank accession numbers/the gene locus names for rice XATs discussed in this study are OK632045/Os02g22480/Os02g0330200 for OsXAT2, OK632046/Os03g37010/Os03g0567600 for OsXAT3, OK632047/Os06g49320/Os06g0707200 for OsXAT4, OK632048/Os02g04250/Os02g0135500 for OsXAT5, OK632049/Os10g35020/Os10g0492200 for OsXAT6, OK632050/Os01g72610/Os01g0956200 for OsXAT7. The GenBank accession numbers for the other grass genes discussed in this study are OK632051 for ZmXAT1, OK632052 for ZmXAT2, OK632053 for SbXAT1, OK632054 for BdXAT1, OK632055 for PvXAT1, OK632056 for PvXAT2, OK632057 for PvXAT3, MG763173 for OsXYXT1, OK632058 for ZmXYXT1, OK632059 for SbXYXT1, OK632060 for BdXYXT1, OK632061 for PvXYXT1, and OK632062 for PvXYXT2.

Results

Identification of new rice GT61 members involved in 3-*O*-arabinosylation of xylan

Four members in clade A of the rice GT61 family, including OsXAT2/3, XAX1 and XYXT1, have been previously shown to be involved in xylan substitutions (Anders et al. 2012; Chiniquy et al. 2012; Zhong et al. 2018b). To investigate the potential roles of the other members of the rice GT61 family (Fig. 1A) in xylan substitutions, we employed the gain-of-function approach to heterologously express the rest 15 clade A members and all 5 clade B members in the Arabidopsis *gux1/2/3* mutant. Xylan from transgenic

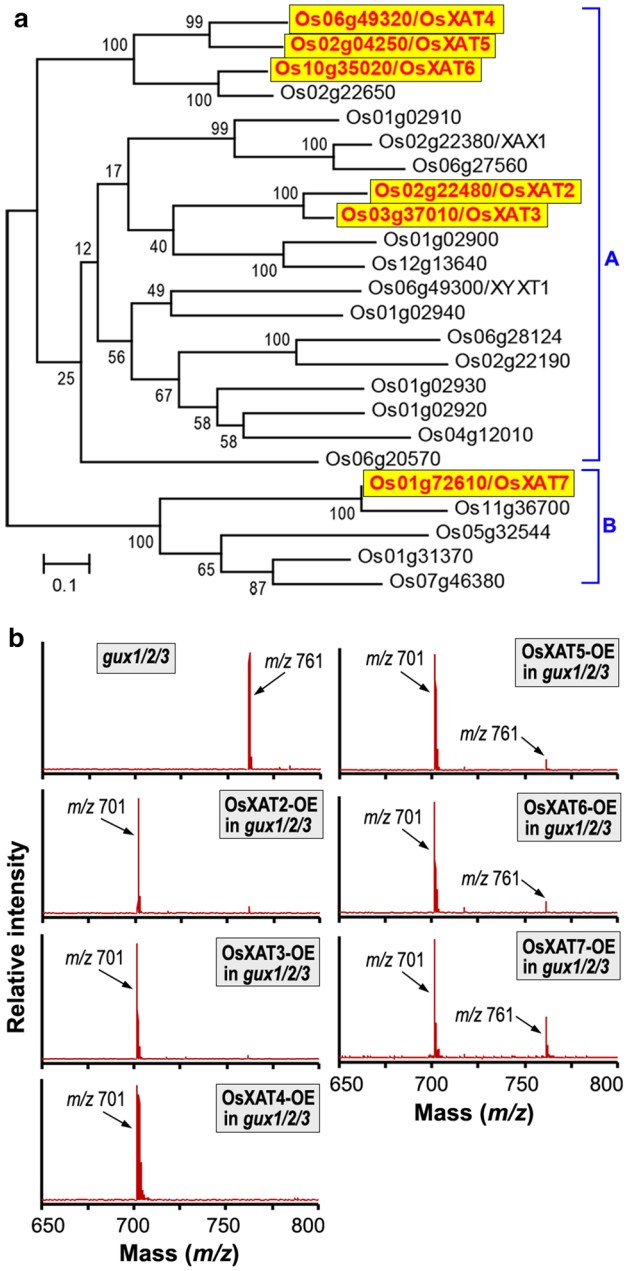

Fig. 1 MALDI-TOF mass spectrometry of xylanase-released xylo-oligomers from xylan of transgenic *gux1/2/3* expressing rice GT61 genes. **a** Phylogenetic relationship of members in clades A and B of the rice GT61 family. Highlighted in yellow are the four newly identified OsXAT4/5/6/7 and the two previously reported OsXAT2/3. The phylogenetic tree was constructed using the maximum likelihood method and the bootstrap values from 1000 replicates are shown as percentages at the nodes. The 0.1 scale denotes 10% change. **b** MALDI-TOF mass spectra showing the appearance of a new ion species at *m/z* 701 ($[M+Na]^+$) in the xylooligomers from transgenic *gux1/2/3* expressing OsXATs compared with those from the *gux1/2/3* mutant. The ion species at *m/z* 761 corresponds to the pentasaccharide reducing end sequence of xylan

gux1/2/3 expressing these rice GT61 genes was digested with the GH11 xylanase to release xylooligomers, which were examined for their structure. The GH11 xylanase hydrolyzes the unsubstituted xylan backbone into Xyl monomers and dimers, whereas its digestion of xylan decorated with side chains produces substituted xylooligomers since it is unable to cleave the xylosidic bond between a substituted Xyl and an unsubstituted Xyl (Paes et al. 2012). Mutations of the Arabidopsis *GUX1/2/3* genes cause a complete lack of GlcA/MeGlcA side chains in xylan (Mortimer et al. 2010; Lee et al. 2012) and as expected, MALDI-TOF mass spectrometry of xylooligomers generated from xylanase digestion of xylan of the *gux1/2/3* mutant only showed ion species at *m/z* 761 and 629 corresponding to the xylan reducing end sequence, Xyl-Xyl-Rha-GalA-Xyl and Xyl-Rha-GalA-Xyl, respectively, due to digestion of the unsubstituted xylan backbone into Xyl monomers/dimers (Fig. 1B; Supplementary Fig. S1). By contrast, MALDI-TOF mass spectrometry of xylooligomers from xylan of transgenic *gux1/2/3* expressing rice GT61 genes revealed that like that of OsXAT2/3, expression of four previously uncharacterized rice GT61 members resulted in a new prominent ion species at *m/z* 701 corresponding to oligomers with five pentosyl residues (Fig. 1B). The appearance of the *m/z* 701 ion species indicates that xylan from these transgenic *gux1/2/3* was substituted, which prevented the digestion of the xylan backbone into Xyl monomers/dimers by xylanase. Since these four rice GT61 members were later found to add Ara*f* residues onto xylan (see below), they were named OsXAT4 (Os06g49320), OsXAT5 (Os02g04250), OsXAT6 (Os10g35020) and OsXAT7 (Os01g72610).

The *m/z* 701 ion species in the xylooligomers from *gux1/2/3* expressing these GT61 members is most likely attributed to xylotetraose substituted with a pentosyl residue, Ara*f* or Xyl. We next employed ^{1}H NMR spectroscopy to determine the chemical structure of these xylooligomers. While the xylooligomers from the *gux1/2/3* mutant displayed major resonances that are characteristic of the xylan reducing end sequence, those from *gux1/2/3* expressing these GT61 genes exhibited predominant resonances attributed to xylan backbone Xyl residues, including H1 of reducing α-Xyl at 5.18 ppm, H1 of reducing β-Xyl at 4.58 ppm and H1 of unbranched β-Xyl at 4.45 ppm (Fig. 2; Supplementary Table S1). More importantly, similar to those from *gux1/2/3*

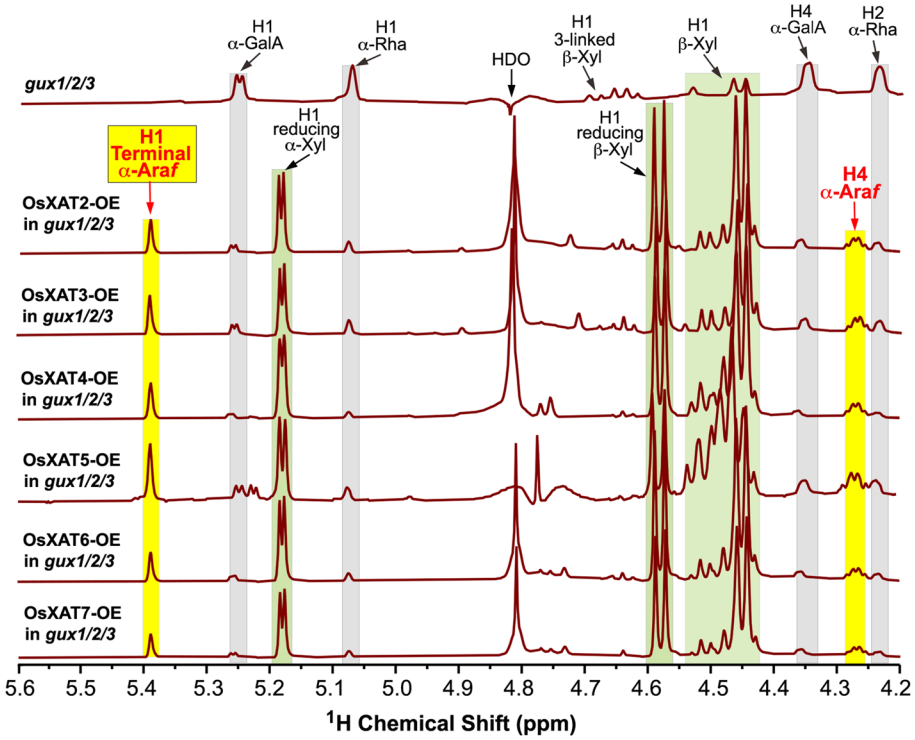

Fig. 2 ^{1}H NMR spectroscopy of xylooligomers from xylan of transgenic *gux1/2/3* expressing rice GT61 genes. The resonance peaks are marked with the proton positions and the corresponding residue identities. Note the appearance of resonances corresponding to H1 of 3-*O*-linked terminal α-Ara*f* at 5.39 ppm and H4 of α-Ara*f* at 4.27 ppm (highlighted in yellow) in the xylooligomers from *gux1/2/3* expressing OsXATs compared with those from *gux1/2/3*. The resonances attributed to the xylan reducing end sequence are H1 of α-GalA at 5.26 ppm, H1 of α-Rha at 5.08 ppm, H1 of 3-linked β-Xyl at 4.67 ppm, H4 of α-GalA at 4.36 ppm, and H2 of α-Rha at 4.23 ppm (highlighted in gray). The resonances corresponding to the xylan backbone Xyl residues are H1 of reducing α-Xyl at 5.18 ppm, H1 of reducing β-Xyl at 4.58 ppm, and H1 of β-Xyl at 4.42–4.54 ppm (highlighted in green). *HDO* hydrogen deuterium oxide

expressing OsXAT2/3, the xylooligomers from *gux1/2/3* expressing OsXAT4/5/6/7 also showed a diagnostic resonance at 5.39 ppm corresponding to H1 of terminal α-Ara*f* attached to *O*-3 of backbone Xyl residues (Fig. 2; Höije et al. 2006), indicating that the xylooligomers from *gux1/2/3* expressing OsXAT4/5/6/7 were substituted with 3-*O*-Ara*f* residues. In addition, the resonances at 4.26 ppm corresponding to H4 of α-Ara*f* were also evident (Fig. 2), further supporting the presence of Ara*f* side chains in the xylooligomers from *gux1/2/3* expressing OsXAT4/5/6/7. These results demonstrated that like OsXAT2/3, OsXAT4/5/6/7 were able to add 3-*O*-Ara*f* side chains onto xylan when heterologously expressed in the Arabidopsis *gux1/2/3* mutant, suggesting that they are most likely xylan 3-*O*-arabinosyltransferases. It was noticed that a few minor unknown peaks were present in some of the spectra of xylooligomers from *gux1/2/3* expressing these OsXAT genes, which did not appear to match with any known chemical shifts of glycosyl residues in xylan. Due to their low abundance, it was impossible to determine their structure and thus, their identities remain unknown.

OsXAT4/5/6/7 are Golgi-localized xylan arabinosyltransferases

We next examined whether these putative OsXATs were localized in the Golgi, where xylan biosynthesis occurs. It was found that their GFP-tagged proteins were co-localized with mCherry-tagged FRA8 (Fig. 3), a known Golgi-localized glycosyltransferase involved in xylan synthesis (Zhong et al. 2005). Although OsXAT2/3 were previously shown to arabinosylate xylan when expressed in Arabidopsis (Anders et al., 2012), only OsXAT2 was biochemically confirmed to be a xylan 3-*O*-arabinosyltransferase (Zhong et al. 2018b). To ascertain whether OsXAT3 and the four newly identified OsXATs are xylan arabinosyltransferases, we expressed their recombinant proteins in HEK293 cells for biochemical characterization. These OsXATs were predicted to be type II membrane proteins with an N-terminal transmembrane helix followed by a putative catalytic domain (Supplementary Fig. S2). The recombinant proteins of these OsXATs without the N-terminal transmembrane helix were successfully generated (Fig. 4A) and their arabinosyltransferase activities were examined by incubation with UDP-Ara*f* and the anthranilic acid (AA)-labeled xylohexaose (X_6-AA) acceptors. MALDI-TOF mass spectrometry of the reaction products revealed that in addition to the X_6-AA acceptor at *m/z* 954, there appeared up to three new ion species at *m/z* 1086, 1218 and 1350 (Fig. 4B), which had a successive mass increment of 132 Da (corresponding to one Ara*f* residue) over the mass of the X_6-AA acceptor, indicating that they are mono-, di, and tri-arabinosylated X_6-AA, respectively. While OsXAT3/4/7 only added one Ara*f* residue onto X_6-AA, OsXAT6 could add up to two and OsXAT2/5 up to three Ara*f* residues (Fig. 4B). Together with the *in planta* data (Figs. 1 and 2), these results established that like OsXAT2, OsXAT3/4/5/6/7 are xylan 3-*O*-arabinosyltransferases.

We further investigated the minimal length of xylooligomers required by OsXATs for arabinosylation. Since OsXAT2/5 exhibited the highest activities toward the X_6-AA acceptors (Fig. 4B), they were tested to arabinosylate AA-labeled xylooligomers with different degrees of polymerization (DP), including xylotriose (X_3), xylotetraose (X_4) and xylopentaose (X_5). MALDI-TOF mass spectrometry of the reaction products showed that xylooligomers with a DP of as low as 3 were efficiently mono-arabinosylated by both OsXAT2 and OsXAT5 (Fig. 5). Although X_6-AA was readily di-arabinosylated by both OsXAT2 and OsXAT5 (Fig. 4B), significant di-arabinosylation of xylooligomers with a lower DP was only observed on X_5-AA in the OsXAT5-catalyzed reaction (Fig. 5C), indicating that di-arabinosylation by OsXAT2/5 is dependent on the DP of the xylooligomer acceptors.

The OsXAT genes display differential expression patterns in different organs

The finding that multiple OsXATs could add Ara*f* residues onto xylan prompted us to find out whether they were differentially expressed in different organs. The spatio-temporal expression data of OsXAT genes in various tissues and organs throughout the plant growth cycle were retrieved from the Rice Expression Profile Database (http://ricexpro.dna.affrc.go.jp/GGEP/) and comparison of these data showed a notable difference in the expression of OsXATs in different organs (Supplementary Fig. S3). It was evident that *OsXAT3/4/5/7* displayed predominant expression in leaf sheath, roots, and except for *OsXAT7*, stems. *OsXAT3/5/7* had a higher expression in leaf blades than other OsXATs. The OsXAT genes were also differentially expressed in various reproductive organs (Supplementary Fig. S3). These data suggest that the Ara*f* substitutions of xylan in different rice organs are likely catalyzed by a combination of different OsXATs.

A number of OsXAT homologs from maize, sorghum, *Brachypodium* and switchgrass exhibit xylan arabinosyltransferase activities

A common feature of grass xylan is its extensive substitutions with 3-*O*-Ara*f* (Vogel 2008). To further our understanding of xylan arabinosylation in grass species, we BLAST-searched the genomes of maize, sorghum, *Brachypodium* and switchgrass and found a number of close homologs of OsXATs (Fig. 6A). Attempts to express the recombinant proteins of these grass XAT homologs in

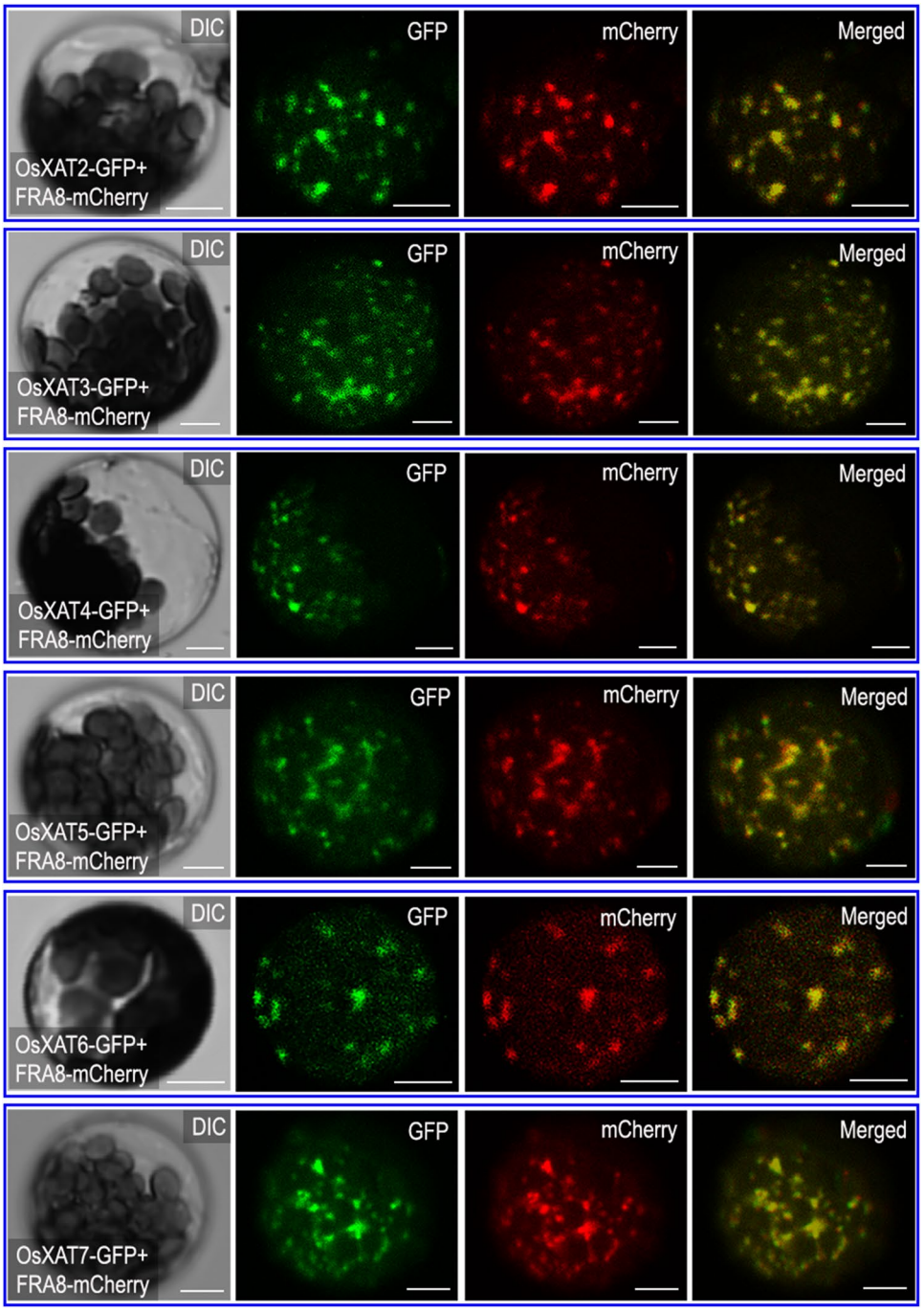

Fig. 3 Subcellular localization of OsXATs. Constructs encoding OsXATs tagged with GFP (OsXAT-GFP) and FRA8-mCherry were co-transfected into Arabidopsis protoplasts and the transfected cells were imaged for GFP and mCherry signals using a confocal microscope. DIC, differential interference contrast. The merged images are overlays of the GFP and mCherry signals. Note the co-localization of the punctate signals of OsXAT-GFP with those of the Golgi-localized FRA8-mCherry. Scale bars = 8.8 µm

HEK293 cells led to the production of several of them, including two from maize, one each from sorghum and *Brachypodium*, and three from switchgrass (Fig. 6B). Arabinosyltransferase activity assays by incubation with UDP-Ara*f* and the X_6-AA acceptors followed by MALDI-TOF mass spectrometry revealed that while ZmXAT2 and SbXAT1 could transfer one Ara*f* residue onto X_6-AA, ZmXAT1, BdXAT1 and PvXAT1/2/3 were able to add up to two Ara*f* residue onto X_6-AA (Fig. 6B), indicating the functional conservation of these XAT homologs as xylan arabinosyltransferases in grass species.

XYXT homologs from maize, sorghum, *Brachypodium* and switchgrass are able to add 2-*O*-Xyl side chains onto xylan

One of the rice GT61 members, OsXYXT1, has previously been demonstrated to be a xylan 2-*O*-xylosyltransferase

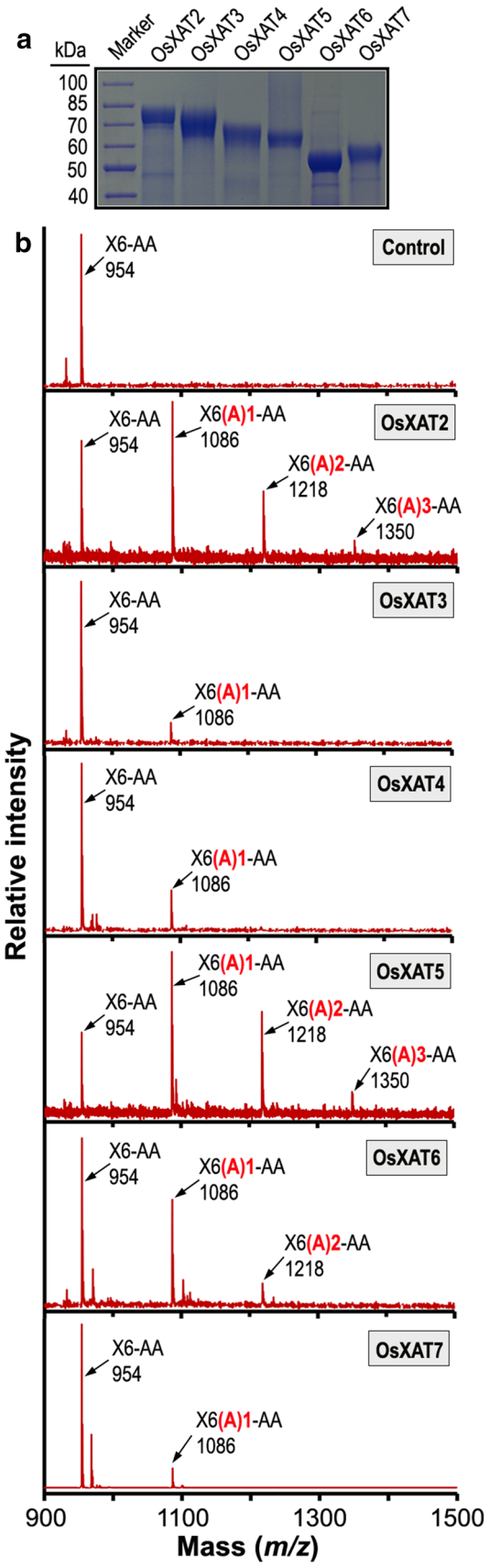

Fig. 4 Detection of the arabinosyltransferase activities of OsXATs. **a** SDS-PAGE and Coomassie Blue staining of the recombinant OsXAT2/3/4/5/6/7 proteins expressed in HEK293 cells. The molecular masses of markers (kDa) are shown on the left. **b** MALDI-TOF mass spectra of OsXAT-catalyzed reaction products. OsXATs were incubated with UDP-Ara*f* and the anthranilic acid (AA)-labeled xylohexaose (X_6-AA) acceptors, and the reaction products were examined with MALDI-TOF mass spectrometry. The control was heat-denatured OsXAT2 incubated with UDP-Ara*f* and X_6-AA. Each ion species is denoted with its mass ($[M+Na]^+$) and oligomer composition. The ion species at *m/z* 954 corresponds to the X_6-AA acceptor and those at *m/z* 1086, 1218 and 1350 have a successive mass increment of 132 Da (corresponding to one Ara*f* residue) over the mass of X_6-AA and are attributed to X_6-AA decorated with one Ara*f* [$X_6(A)_1$-AA], two Ara*f* [$X_6(A)_2$-AA] and three Ara*f* [$X_6(A)_3$-AA], respectively

catalyzing the addition of 2-*O*-Xyl side chains onto the xylan backbone (Zhong et al. 2018b). It is currently unknown whether other grass species also harbor xylan 2-*O*-xylosyltransferases involved in decorating the xylan backbone with 2-*O*-Xyl side chains. A BLAST search revealed the presence of XYXT close homologs in the genomes of several grass species, including maize, sorghum, *Brachypodium* and switchgrass (Fig. 7A). To find out whether these grass XYXT homologs possess xylan 2-*O*-xylosyltransferase activities, we first tried to express them in HEK293 cells but failed to obtain any recombinant proteins, and hence we resorted to the gain-of-function approach to express them in the Arabidopsis *gux1/2/3* mutant. Xylooligomers released by xylanase digestion of xylan from *gux1/2/3* expressing these grass XYXT homologs were examined for their structure and compared with those from the *gux1/2/3* mutant. MALDI-TOF mass spectrometry revealed that although the xylooligomers from *gux1/2/3* only had the *m/z* 761 ion species attributed to the xylan reducing end pentasaccharide sequence, those from *gux1/2/3* expressing grass XYXTs displayed a prominent ion species at *m/z* 701 corresponding to xylotetraose substituted with a pentosyl residue (Fig. 7B), indicating that xylan from these transgenic *gux1/2/3* was substituted.

Structural analysis using ^{1}H NMR spectroscopy showed that while the xylooligomers from *gux1/2/3* only had resonances attributed to the xylan reducing end sequence, those from *gux1/2/3* expressing grass XYXTs exhibited predominant resonances that are characteristic of xylan backbone Xyl residues (Fig. 7C), further indicating that xylan from these transgenic *gux1/2/3* was substituted. The presence of prominent resonances at 4.64 ppm (Fig. 7C), which were attributed to 2-*O*-Xyl side chains of xylan (Zhong et al. 2018b), suggests that xylan from these transgenic *gux1/2/3* was substituted with 2-*O*-Xyl residues.

Since the resonances for 2-*O*-Xyl side chains and branched backbone Xyl residues were partially overlapped in the 1D NMR spectra, we next applied 2D NMR

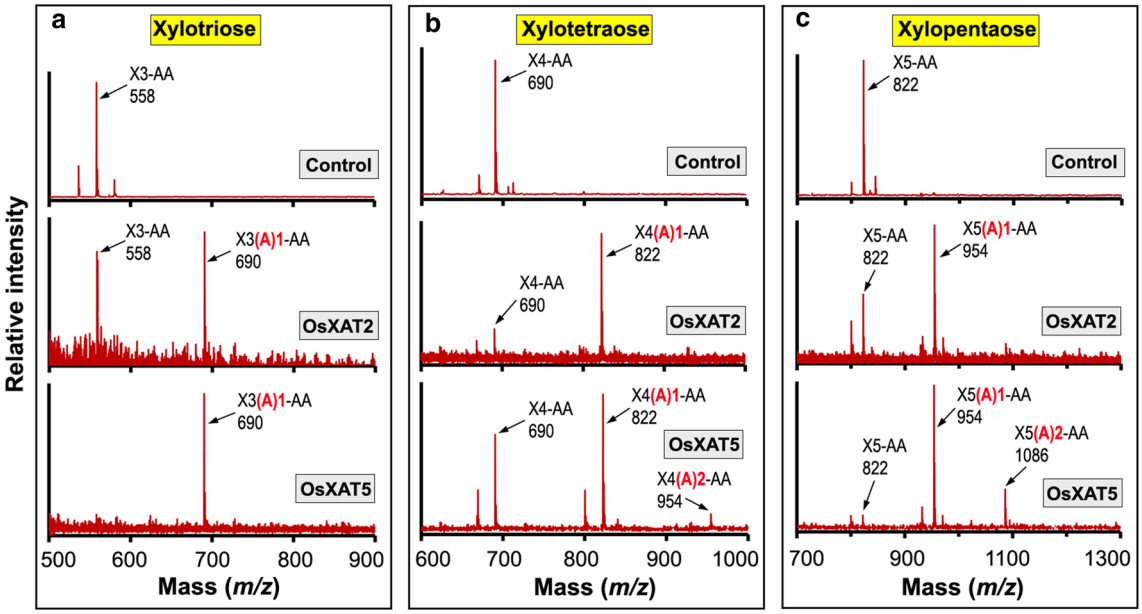

Fig. 5 Arabinosyltransferase activities of OsXAT2/5 toward xylooligomers with different degrees of polymerization. OsXAT2/5 were incubated with UDP-Ara*f* and the indicated xylooligomer acceptors, and the reaction products were examined with MALDI-TOF mass spectrometry. Each ion species is denoted with its mass ($[M+Na]^+$) and oligomer composition. **a** MALDI-TOF mass spectra of the reaction products of AA-labeled xylotriose (X_3-AA) incubated with heat-denatured OsXAT2 (top), OsXAT2 (middle) or OsXAT5 (bottom). The ion species at *m/z* 558 corresponds to the X_3-AA acceptor and that at *m/z* 690 has a mass increment of 132 Da (corresponding to one Ara*f* residue) over the mass of X_3-AA and is attributed to X_3-AA decorated with one Ara*f* residue [$X_3(A)_1$-AA]. **b** MALDI-TOF mass spectra of the reaction products of AA-labeled xylotetraose (X_4-AA) incubated with heat-denatured OsXAT2 (top), OsXAT2 (middle) or OsXAT5 (bottom). The ion species at *m/z* 690 corresponds to the X_4-AA acceptor and those at *m/z* 822 and 954 have a successive mass increment of 132 Da over the mass of X_4-AA and are attributed to X_4-AA decorated with one Ara*f* [$X_4(A)_1$-AA] and two Ara*f* [$X_4(A)_2$-AA], respectively. **c** MALDI-TOF mass spectra of the reaction products of AA-labeled xylopentaose (X_5-AA) incubated with heat-denatured OsXAT2 (top), OsXAT2 (middle) or OsXAT5 (bottom). The ion species at *m/z* 822 corresponds to the X_5-AA acceptor and those at *m/z* 954 and 1086 have a successive mass increment of 132 Da over the mass of X_5-AA and are attributed to X_5-AA decorated with one Ara*f* [$X_5(A)_1$-AA] and two Ara*f* [$X_5(A)_2$-AA], respectively

spectroscopy, including heteronuclear single quantum coherence (HSQC) and heteronuclear multiple bond correlation (HMBC), to verify the presence of 2-*O*-Xyl side chains in the xylooligomers (Fig. 8A) from *gux1/2/3* expressing grass XYXTs. The HSQC analysis, which provides correlation between each carbon and its attached protons, showed that the spectral region of the one-bond H1–C1 anomeric correlation exhibited distinct resonances corresponding to the Xyl5 side-chain residue (the correlation between H1 of β-Xyl5 at 4.640 ppm and C1 of β-Xyl5 at 103.6 ppm) and the branched Xyl3 residue (the correlation between H1 of β-Xyl3 at 4.635 ppm and C1 of β-Xyl3 at 100.1 ppm) (Figs. 8 and 9), verifying that the resonances at 4.64 ppm observed on the 1D NMR spectra were attributed to the Xyl side chains. The HMBC analysis, which provides correlations between carbons and protons that are separated by two bonds or more, revealed resonances corresponding to the correlation between H1 of β-Xyl5 at 4.640 ppm and C2 of β-Xyl3 at 80.3 ppm as well as the correlation between H2 of β-Xyl3 at 3.520 ppm and C1 of β-Xyl5 at 103.6 ppm (Figs. 8 and 9), further supporting that the Xyl5 side-chain residue is attached to Xyl3 at *O*-2. The HMBC spectra also displayed resonances attributed to the correlation between H1 of β-Xyl2 at 4.460 ppm and C4 of β-Xyl1 at 76.3 ppm, that between H1 of β-Xyl3 (4.635 ppm) and C4 of β-Xyl2 (76.3 ppm), and that between H1 of β-Xyl4 (4.460 ppm) and C4 of β-Xyl3 (76.3 ppm) in the xylan backbone. These results confirmed that xylan from *gux1/2/3* expressing grass XYXTs was substituted at *O*-2 with β-Xyl side chains, indicating that these XYXTs are functionally conserved in mediating the transfer of 2-*O*-Xyl side chains onto the xylan backbone.

Discussion

Grass xylan differs from dicot xylan by having extensive Ara*f* substitutions. The Ara*f* side chains in grass xylan could be further substituted with hydroxycinnamates that are involved in crosslinking xylan with lignin, which contributes to biomass recalcitrance in grass species (Vogel 2008). Therefore, characterization of genes responsible

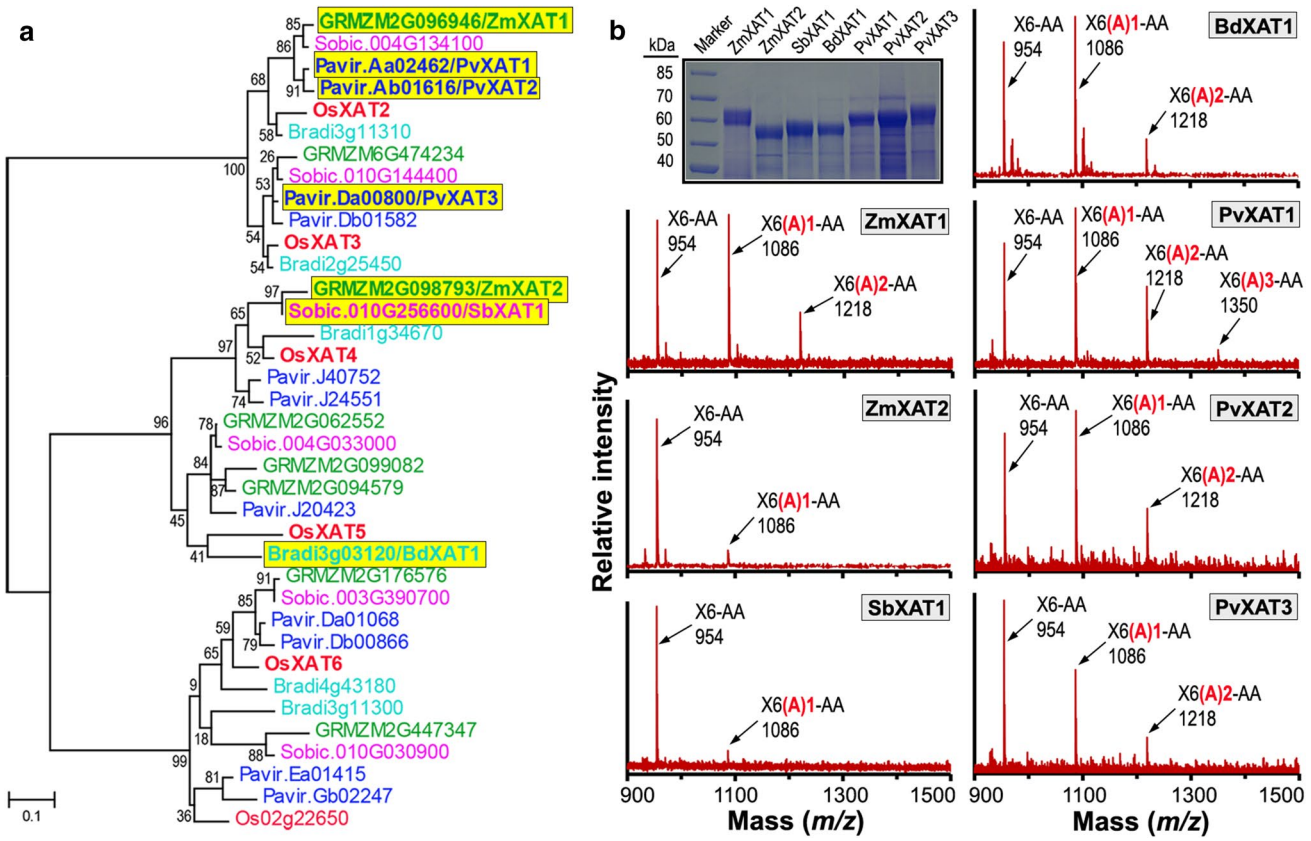

Fig. 6 Identification of xylan arabinosyltransferases in other grass species. **a** Phylogenetic analysis of the close homologs of OsXAT2/3/4/5/6 in other grass species, including maize (GRMZM/Zm), sorghum (Sobic/Sb), *Brachypodium distachyon* (Bradi/Bd) and switchgrass (Pavir/Pv). The phylogenetic tree was constructed using the maximum likelihood method and the bootstrap values from 1000 replicates are shown as percentages at the nodes. The 0.1 scale denotes 10% change. **b** MALDI-TOF mass spectrometry of the reaction products catalyzed by grass XATs. Shown at the top left panel is the SDS-PAGE and Coomassie Blue staining of the recombinant grass XATs expressed in HEK293 cells. The molecular masses of markers (kDa) are shown on the left. XATs were incubated with UDP-Ara*f* and the AA-labeled xylohexaose (X_6-AA) acceptors and the reaction products were examined with MALDI-TOF mass spectrometry. Each ion species is denoted with its mass ($[M+Na]^+$) and oligomer composition. The ion species at *m/z* 954 corresponds to the X_6-AA acceptor and those at *m/z* 1086, 1218 and 1350 are attributed to X_6-AA decorated with one Ara*f* [$X_6(A)_1$-AA], two Ara*f* [$X_6(A)_2$-AA] and three Ara*f* [$X_6(A)_3$-AA], respectively

for xylan arabinosylation could have significant biotechnological implications. Despite the importance of Ara*f* substitutions in xylan, our understanding of xylan arabinosylation in grass species is still limited. So far, only four GT61 members, TaXAT1/2 from wheat and OsXAT2/3 from rice, have been implicated in xylan arabinosylation (Anders et al. 2012) and among them, only OsXAT2 was biochemically proven to be a xylan arabinosyltransferase (Zhong et al. 2018b). In this report, we have found four new rice GT61 members, OsXAT4/5/6/7, that are capable of arabinosylating xylan at *O*-3 when heterologously expressed in the Arabidopsis *gux1/2/3* mutant. Furthermore, we demonstrated that like OsXAT2, the recombinant proteins of OsXAT3/4/5/6/7 were able to transfer Ara*f* residues onto the xylohexaose acceptors, which provides biochemical evidence that these rice GT61 members are xylan arabinosyltransferases.

The finding of four new rice GT61 members as xylan 3-*O*-arabinosyltransferases suggests that they are also involved in xylan arabinosylation in rice besides OsXAT2/3. This proposition is consistent with the observation that simultaneous mutations of the *OsXAT2* and *OsXAT3* genes resulted in only about 30% reduction in the arabinosyl level in rice cell walls (Chen et al. 2021). The differential expression of OsXAT genes in different organs (Supplementary Fig. S3) indicates that different OsXATs are involved in xylan arabinosylation in different organs. Other grass species, such as maize, sorghum, *Brachypodium* and switchgrass, also harbor multiple XAT homologs and several of them were demonstrated to be xylan arabinosyltransferases in this study. Since genetic alterations of xylan Ara*f* side chains in rice was shown to increase saccharification efficiency (Sumiyoshi et al. 2013; Chen et al. 2021), our identification of several XATs in the biofuel crop switchgrass

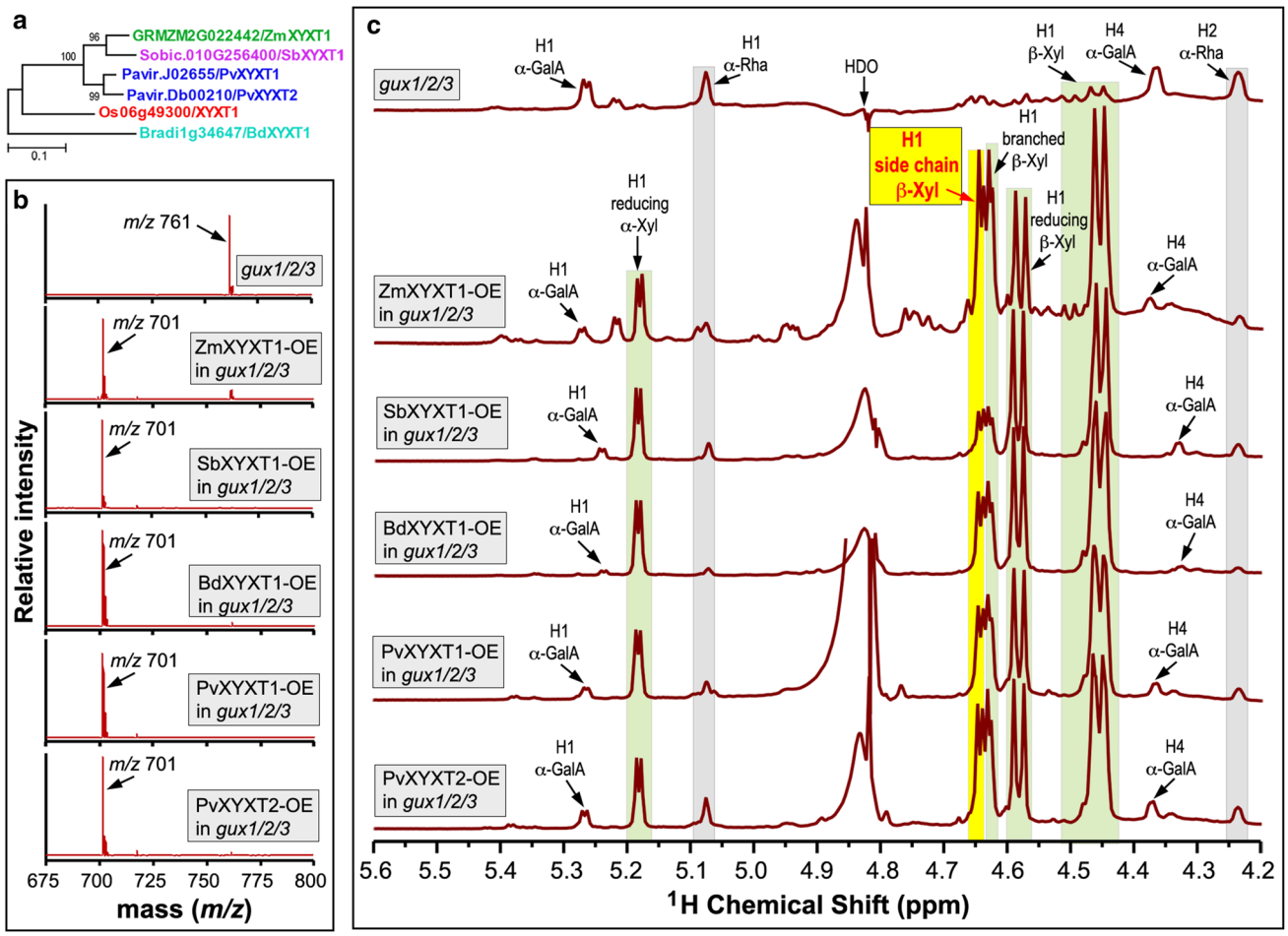

Fig. 7 Structure analysis of xylanase-released xylooligomers from xylan of transgenic *gux1/2/3* expressing grass XYXTs. **a** Phylogenetic analysis of XYXT homologs from rice (Os), maize (Zm), sorghum (Sb), *Brachypodium distachyon* (Bd) and switchgrass (Pv). The phylogenetic tree was constructed using the maximum likelihood method. The bootstrap values from 1000 replicates are shown as percentages at the nodes and the 0.1 scale denotes 10% change. **b** MALDI-TOF mass spectrometry of xylooligomers from *gux1/2/3* expressing grass XYXTs. Note the appearance of a new ion species at *m/z* 701 ($[M+Na]^+$) in the xylooligomers from these transgenic *gux1/2/3* compared with those from *gux1/2/3*. The ion species at *m/z* 761 corresponds to the reducing end pentasaccharide sequence of xylan. **c** ^{1}H NMR spectroscopy of xylooligomers from *gux1/2/3* expressing grass XYXTs. The resonance peaks are marked with the proton positions and the corresponding residue identities. Note the presence of resonances corresponding to side-chain Xyl residues at 4.64 ppm (highlighted in yellow) in the xylooligomers from *gux1/2/3* expressing grass XYXTs compared with those from *gux1/2/3*. The resonances attributed to the xylan reducing end sequence are highlighted in gray, and those corresponding to the xylan backbone Xyl residues are highlighted in green. The chemical shifts of α-GalA exhibited some slight variations due to its acidic nature. HDO, hydrogen deuterium oxide

provides molecular tools for genetic manipulation of xylan arabinosylation for potential improvement of its biomass saccharification.

The previously identified GT61 members involved in grass xylan substitutions reside in clade A, which had undergone a substantial expansion in grass species (Anders et al. 2012). It is important to note that among the four newly identified OsXATs reported in this study, OsXAT7 resides in clade B, which did not exhibit any expansion in grass species. The finding that a clade B GT61 member is a xylan 3-*O*-arabinosyltransferase expands our understanding of the functional roles of family GT61 members in xylan substitutions. It was shown that in Arabidopsis, mutation of a clade B GT61 member, MUCI21 (mucilage-related 21), caused a reduction in 2,4-linked Xyl residues in seed mucilage and thus it was proposed to be essential for the synthesis of highly branched xylan in seed mucilage by facilitating addition of Xyl residues directly onto the xylan backbone (Voiniciuc et al. 2015). However, its heterologous expression in the Arabidopsis *gux1/2/3* mutant did not lead to xylosyl substitution of the xylan backbone (Zhong et al. 2018b), and therefore its exact function remains elusive.

Besides the predominant Ara*f* substituents, other minor ones, such as GlcA/MeGlcA residues, are present in grass

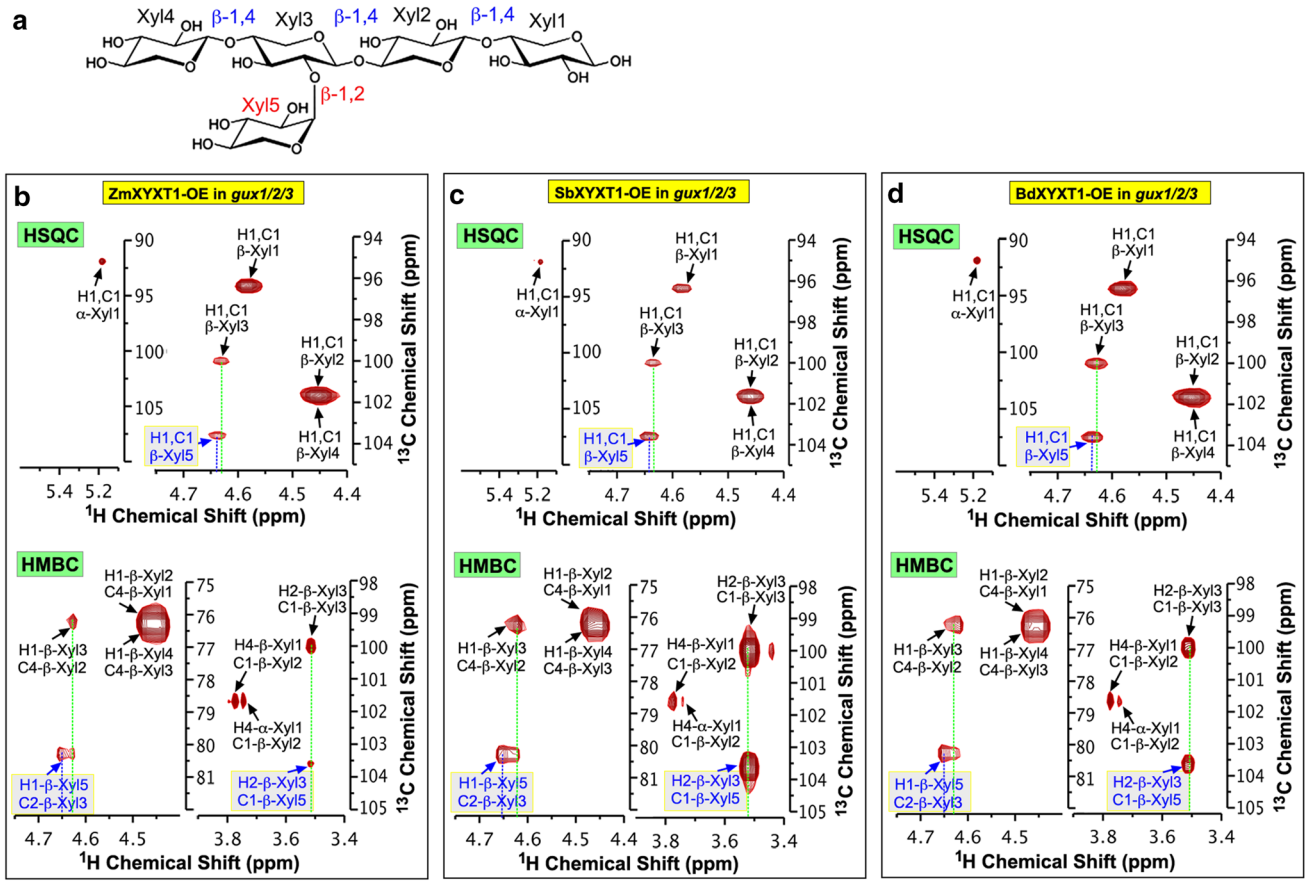

Fig. 8 Two-dimensional NMR analysis of the glycosidic linkages of xylooligomers from *gux1/2/3* expressing XYXTs from maize, sorghum and *Brachypodium*. **a** Diagram of the structure of a xylooligomer from xylan of *gux1/2/3* expressing grass XYXTs. The numbering of the Xyl residues used for explanation of the NMR data in **b**–**d** is indicated. **b**–**d** HSQC (top panels) and HMBC (bottom panels) spectra of xylooligomers from *gux1/2/3* expressing ZmXYXT1 (**b**), SbXYXT1 (**c**) and BdXYXT1 (**d**). The HSQC spectra display the one-bond H1–C1 correlations between ^{1}H and ^{13}C of each Xyl and the HMBC spectra show interglycosidic cross peaks between ^{1}H and ^{13}C. Note the H1–C1 signals of the side-chain Xyl5 at 4.64 ppm (^{1}H) and 103.6 ppm (^{13}C) (top panels) and the cross-peak signals between H1 of Xyl5 at 4.64 ppm and C2 of Xyl3 at 80.3 ppm and those between H2 of Xyl3 at 3.520 ppm and C1 of Xyl5 at 103.6 ppm (bottom panels)

xylan (Vogel 2008). Rice xylan may also be directly substituted with Xyl side chains since a rice xylan 2-*O*-xylosyltransferase, OsXYXT1, was shown to be able to transfer 2-*O*-Xyl residues directly onto the xylan backbone (Zhong et al. 2018b). Although 2-*O*-Xyl substituents on the xylan backbone have not been reported in grasses probably due to their low abundance, they were found on the backbone of xylan from the seed mucilage of *Plantago ovata* (Fischer et al. 2004). The seed mucilage of *Plantago* species has been shown to be predominantly composed of Ara*f*-substituted xylan and the expression of several members of the GT61 family is elevated during seed mucilage production (Jensen et al. 2013; Phan et al. 2016). Our finding that like OsXYXT1, XYXT homologs from maize, sorghum, *Brachypodium* and switchgrass were able to add 2-*O*-Xyl residues onto the xylan backbone when heterologously expressed in the Arabidopsis *gux1/2/3* mutant provides additional lines of evidence suggesting that 2-*O*-Xyl substitutions on the xylan backbone may be common in grasses. Further functional investigation of family GT61 glycosyltransferases will yield additional new insights into their roles in xylan biosynthesis in grass species.

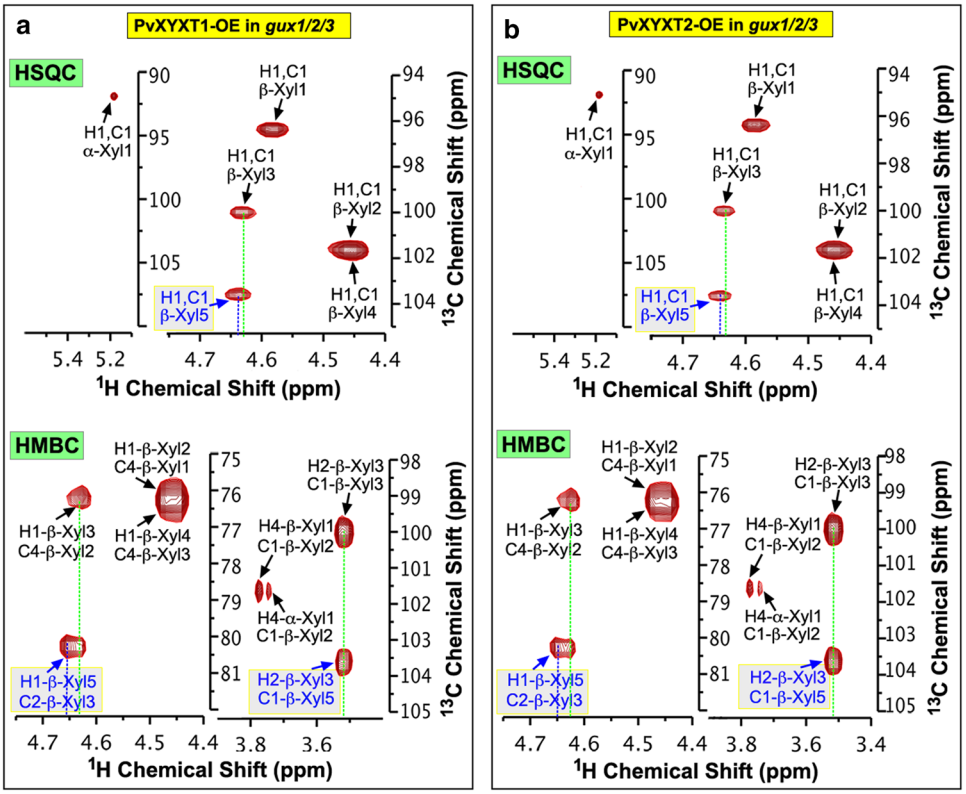

Fig. 9 HSQC and HMBC spectra of xylooligomers from xylan of *gux1/2/3* expressing switchgrass XYXTs. The numbering of the Xyl residues is the same as that shown in Fig. 8a. Note the H1–C1 signals of the side-chain Xyl5 at 4.64 ppm (^{1}H) and 103.6 ppm (^{13}C) (top panels) and the cross-peak signals between H1 of Xyl5 at 4.64 ppm and C2 of Xyl3 at 80.3 ppm and those between H2 of Xyl3 at 3.520 ppm and C1 of Xyl5 at 103.6 ppm (bottom panels)

Author contribution statement RZ and ZHY conceived and designed research. RZ, DC, DRP, NTS and ZHY conducted experiments and analyzed data. RZ and ZHY wrote the manuscript. All authors read and approved the manuscript.

Supplementary Information The online version contains supplementary material available at https://doi.org/10.1007/s00425-021-03794-y.

Acknowledgements This work was funded by the U.S. Department of Energy, Office of Science, Office of Basic Energy Sciences [grant No. DE-FG02-03ER15415]. NTS was grateful to the UGA Plant Biology Undergraduate Research Award. We thank the UGA Proteomics and Mass Spectrometry Core Facility for assistance with MALDI using the Bruker Autoflex mass spectrometer and Dr. M.K. Kandasamy at the UGA Biomedical Microscopy Core for assistance with imaging using the Zeiss LSM 710 confocal microscope.

Data availability All data generated during this study are included in this article and its Supplementary Figure files.

References

Anders N, Wilkinson MD, Lovegrove A, Freeman J, Tryfona T, Pellny TK et al (2012) Glycosyl transferases in family 61 mediate arabinofuranosyl transfer onto xylan in grasses. Proc Natl Acad Sci USA 109:989–993

Bartley LE, Peck ML, Kim SR, Ebert B, Manisseri C, Chiniquy DM et al (2013) Overexpression of a BAHD acyltransferase, OsAt10, alters rice cell wall hydroxycinnamic acid content and saccharification. Plant Physiol 161:1615–1633

Buanafina MM (2009) Feruloylation in grasses: current and future perspectives. Mol Plant 2:861–872

Buanafina MM, Fescemyer HW, Sharma M, Shearer EA (2016) Functional testing of a PF02458 homologue of putative rice arabinoxylan feruloyl transferase genes in *Brachypodium distachyon*. Planta 243:659–674

Carvalho DM, Martínez-Abad A, Evtuguin DV, Colodette JL, Lindström ME, Vilaplana F, Sevastyanova O (2017) Isolation and characterization of acetylated glucuronoarabinoxylan from sugarcane bagasse and straw. Carbohydr Polym 156:223–234

Chen C, Zhao X, Wang X, Wang B, Li H, Feng J, Wu A (2021) Mutagenesis of UDP-xylose epimerase and xylan arabinosyltransferase decreases arabinose content and improves saccharification of rice straw. Plant Biotechnol J 19:863–865

Chiniquy D, Sharma V, Schultink A, Baidoo EE, Rautengarten C, Cheng K et al (2012) XAX1 from glycosyltransferase family 61 mediates xylosyltransfer to rice xylan. Proc Natl Acad Sci USA 109:17117–17122

Chiniquy D, Varanasi P, Oh T, Harholt J, Katnelson J, Singh S (2013) Three novel rice genes closely related to the Arabidopsis *IRX9*, *IRX9L*, and *IRX14* genes and their roles in xylan biosynthesis. Front Plant Sci 4:83

de Souza WR, Martins PK, Freeman J, Pellny TK, Michaelson LV, Sampaio BL et al (2018) Suppression of a single BAHD gene in *Setaria viridis* causes large, stable decreases in cell wall feruloylation and increases biomass digestibility. New Phytol 218:81–93

Fanelli A, Rancour DM, Sullivan M, Karlen SD, Ralph J, Riaño-Pachón DM et al (2021) Overexpression of a sugarcane BAHD acyltransferase alters hydroxycinnamate content in maize cell wall. Front Plant Sci 12:626168

Fischer MH, Yu N, Gray GR, Ralph J, Anderson L, Marlett JA (2004) The gel-forming polysaccharide of psyllium husk (*Plantago ovata* Forsk). Carbohydr Res 339:2009–2017

Gao Y, He C, Zhang D, Liu X, Xu Z, Tian Y et al (2017) Two trichome birefringence-like proteins mediate xylan acetylation, which is essential for leaf blight resistance in rice. Plant Physiol 173:470–481

Hartley RD, Morrison WHIII, Himmelsbach DS, Borneman WS (1990) Cross-linking of cell wall phenolic arabinoxylans in graminaceous plants. Phytochemistry 29:3705–3709

Hatfield RD, Rancour DM, Marita JM (2017) Grass cell walls: a story of cross-linking. Front Plant Sci 7:2056

Hoffmann RA, Leeflang BR, de Barse MM, Kamerling JP, Vliegenthart JF (1991) Characterisation by 1H-n.m.r. spectroscopy of oligosaccharides, derived from arabinoxylans of white endosperm of wheat, that contain the elements ->4)[alpha-L-Araf-(1->3)]-beta-D-Xylp-(1-> or ->4)[alpha-L-Araf-(1->2)][alpha- L-Araf-(1->3)]-beta-D-Xylp-(1->. Carbohydr Res 221:63–81

Höije A, Sandstrom C, Roubroeks JP, Andersson R, Gohil S, Gatenholm P (2006) Evidence of the presence of 2-*O*-β-D-xylopyranosyl-α-L-arabinofuranose side chains in barley husk arabinoxylan. Carbohydr Res 341:2959–2966

Ishii T, Ichita J, Matsue H, Ono H, Maeda I (2002) Fluorescent labeling of pectic oligosaccharides with 2-aminobenzamide and enzyme assay for pectin. Carbohydr Res 337:1023–1032

Jensen JK, Johnson N, Wilkerson CG (2013) Discovery of diversity in xylan biosynthetic genes by transcriptional profiling of a heteroxylan containing mucilaginous tissue. Front Plant Sci 4:183

Lee C, Teng Q, Zhong R, Ye Z-H (2012) Arabidopsis GUX proteins are glucuronyltransferases responsible for the addition of glucuronic acid side chains onto xylan. Plant Cell Physiol 53:1204–1216

Lee C, Teng Q, Zhong R, Yuan Y, Ye Z-H (2014) Functional roles of rice glycosyltransferase family GT43 in xylan biosynthesis. Plant Signal Behav 9:e27809

Levetin E, McMahon K (2016) Plant and Society, 7th edn. McGraw-Hill Education, New York

Lovegrove A, Wilkinson MD, Freeman J, Pellny TK, Tosi P, Saulnier L et al (2013) RNA interference suppression of genes in glycosyl transferase families 43 and 47 in wheat starchy endosperm causes large decreases in arabinoxylan content. Plant Physiol 163:95–107

Marriott PE, Gómez LD, McQueen-Mason SJ (2016) Unlocking the potential of lignocellulosic biomass through plant science. New Phytol 209:1366–1381

McCleary BV, McKie VA, Draga A, Rooney E, Mangan D, Larkin J (2015) Hydrolysis of wheat flour arabinoxylan, acid-debranched wheat flour arabinoxylan and arabino-xylo-oligosaccharides by β-xylanase, α-L-arabinofuranosidase and β-xylosidase. Carbohydr Res 407:79–96

Mitchell RA, Dupree P, Shewry PR (2007) A novel bioinformatics approach identifies candidate genes for the synthesis and feruloylation of arabinoxylan. Plant Physiol 144:43–53

Mortimer JC, Miles GP, Brown DM, Zhang Z, Segura MP, Weimar T et al (2010) Absence of branches from xylan in Arabidopsis *gux* mutants reveals potential for simplification of lignocellulosic biomass. Proc Natl Acad Sci USA 107:17409–17414

Mota TR, de Souza WR, Oliveira DM, Martins PK, Sampaio BL, Vinecky F et al (2021) Suppression of a BAHD acyltransferase decreases *p*-coumaroyl on arabinoxylan and improves biomass digestibility in the model grass *Setaria viridis*. Plant J 105:136–150

Naran R, Black S, Decker SR, Azadi P (2009) Extraction and characterization of native heteroxylans from delignified corn stover and aspen. Cellulose 16:661–675

Paes G, Berrin J-G, Beaugrand J (2012) GH11 xylanases: structure/function/properties relationships and applications. Biotechnol Adv 30:564–592

Pellny TK, Lovegrove A, Freeman J, Tosi P, Love CG, Knox JP et al (2012) Cell walls of developing wheat starchy endosperm: comparison of composition and RNA-Seq transcriptome. Plant Physiol 158:612–627

Pellny TK, Patil A, Wood AJ, Freeman J, Halsey K, Plummer A et al (2020) Loss of TaIRX9b gene function in wheat decreases chain length and amount of arabinoxylan in grain but increases cross-linking. Plant Biotechnol J 18:2316–2327

Pena MJ, Zhong R, Zhou G-K, Richardson EA, O'Neill MA, Darvill AG et al (2007) *Arabidopsis irregular xylem8* and *irregular xylem9*: implications for the complexity of glucuronoxylan biosynthesis. Plant Cell 19:549–563

Petrik DL, Tryfona T, Dupree P, Anderson CT (2020) BdGT43B2 functions in xylan biosynthesis and is essential for seedling survival in *Brachypodium distachyon*. Plant Direct 4:e00216

Phan JL, Tucker MR, Khor SF, Shirley N, Lahnstein J, Beahan C et al (2016) Differences in glycosyltransferase family 61 accompany variation in seed coat mucilage composition in *Plantago* spp. J Exp Bot 67:6481–6495

Piston F, Uauy C, Fu L, Langston J, Labavitch J, Dubcovsky J (2010) Down-regulation of four putative arabinoxylan feruloyl transferase genes from family PF02458 reduces ester-linked ferulate content in rice cell walls. Planta 231:677–691

Ralph J, Grabber JH, Hatfield RD (1995) Lignin-ferulate cross-links in grasses: active incorporation of ferulate polysaccharide esters into ryegrass lignins. Carbohydr Res 275:167–178

Sumiyoshi M, Nakamura A, Nakamura H, Hakata M, Ichikawa H, Hirochika H et al (2013) Increase in cellulose accumulation and improvement of saccharification by overexpression of arabinofuranosidase in rice. PLoS One 8:e78269

Urbanowicz BR, Pena MJ, Moniz HA, Moremen KW, York WS (2014) Two Arabidopsis proteins synthesize acetylated xylan *in vitro*. Plant J 80:197–206

Verbruggen MA, Spronk BA, Schols HA, Beldman G, Voragen AG, Thomas JR et al (1998) Structures of enzymically derived oligosaccharides from sorghum glucuronoarabinoxylan. Carbohydr Res 306:265–274

Vogel J (2008) Unique aspects of the grass cell wall. Curr Opin Plant Biol 11:301–307

Voiniciuc C, Günl M, Schmidt MH, Usadel B (2015) Highly branched xylan made by IRREGULAR XYLEM14 and MUCILAGE-RELATED21 links mucilage to Arabidopsis seeds. Plant Physiol 169:2481–2495

Whitehead C, Ostos Garrido FJ, Reymond M, Simister R, Distelfeld A, Atienza SG et al (2018) A glycosyl transferase family 43 protein involved in xylan biosynthesis is associated with straw digestibility in *Brachypodium distachyon*. New Phytol 218:974–985

Yoo SD, Cho YH, Sheen J (2007) Arabidopsis mesophyll protoplasts: a versatile cell system for transient gene expression analysis. Nat Protoc 2:1565–1572

Zeng W, Jiang N, Nadella R, Killen TL, Nadella V, Faik A (2010) A glucurono(arabino)xylan synthase complex from wheat (*Triticum aestivum* L.) contains members of the GT43, 47, and 75 families and functions cooperatively. Plant Physiol 154:78–97

Zhang B, Zhao T, Yu W, Kuang B, Yao Y, Liu T et al (2014) Functional conservation of the glycosyltransferase gene GT47A in the monocot rice. J Plant Res 127:423–432

Zhong R, Peña MJ, Zhou G-K, Nairn CJ, Wood-Jones A, Richardson EA et al (2005) Arabidopsis *Fragile Fiber8*, which encodes a putative glucuronyltransferase, is essential for normal secondary wall synthesis. Plant Cell 17:3390–3408

Zhong R, Cui D, Dasher RL, Ye Z-H (2018a) Biochemical characterization of rice xylan *O*-acetyltransferases. Planta 247:1489–1498

Zhong R, Cui D, Phillips DR, Ye Z-H (2018b) A novel rice xylosyltransferase catalyzes the addition of 2-*O*-xylosyl side chains onto the xylan backbone. Plant Cell Physiol 59:554–565
Zhong R, Cui D, Ye Z-H (2019) Secondary cell wall biosynthesis. New Phytol 221:1703–1723